Electrochimica Acta 112 (2013) 59–67

Contents lists available at ScienceDirect

Electrochimica Acta

journal homepage: www.elsevier.com/locate/electacta

Near infrared electrochromic naphthalene-based polyimides containing triarylamine: Synthesis and electrochemical properties

Jiwei Cai[a,1], Lina Ma[a,1], Haijun Niu[a,*], Ping Zhao[b], Yongfu Lian[a], Wen Wang[c,*]

[a] Key Laboratory of Functional Inorganic Material Chemistry, Ministry of Education, Department of Macromolecular Material and Engineering, School of Chemistry and Chemical Engineering and Materials, Heilongjiang University, Harbin, 150086, PR China
[b] Key Laboratory for Advanced Materials and Institute of Fine Chemicals, East China University of Science and Technology, Shanghai, 200237, PR China
[c] School of Material Science and Engineering, Harbin Institute of Technology, Harbin, 150080, PR China

ARTICLE INFO

Article history:
Received 11 March 2013
Received in revised form 8 June 2013
Accepted 25 August 2013
Available online xxx

Keywords:
Triphenylamine
Electrochromism
Polyimides
Electrochemistry

ABSTRACT

A series of novel multicolored near-infrared (NIR) electrochromic aromatic polyimides (PIs) have been synthesized by a conventional two-step polymerization process. The structures of PIs were characterized by means of Fourier transform infrared (FTIR), ^{1}H NMR spectroscopy, which showed an agreement with the proposed structure. These poly (amic acid)s have inherent viscosities of 0.75–0.84 dl/g. They are readily soluble in many organic solvents, such as N-methyl-2-pyrrolidone (NMP), dimethylacetamide (DMAc), *N,N*-dimethylformamide (DMF) and dimethyl sulfoxide (DMSO). All PIs displayed outstanding thermal stabilities, i.e. 5% wt loss in excess of 480 °C under nitrogen. The highest-occupied molecular orbital (HOMO) and lowest-unoccupied molecular orbital (LUMO) energy levels of these PIs were determined in the range of −4.95 to −5.00 and −1.97 to −2.01 eV (vs the vacuum level) by cyclic voltammetry method which were consisting with the results of quantum chemical calculation well, respectively. All obtained PIs revealed stability of electrochromic characteristics, changing color from original yellowish to red and blue. In addition, the PIs films showed high coloration efficiency (CE), short switching time, and anodic electrochromic behavior. The properties prove that the PIs are multipurpose materials which will be subject of hole-transporting and electrochromic application in the near future.

1. Introduction

Electrochromism is a topic that has attracted a great deal of interest from researchers because of its potential application in various areas (photonics, optics, electronics, architecture) [1–3]. Color changes are commonly required between a transparent state, where the chromophore only absorbs in the UV region, and a colored state or between two colored states in a given electrolyte solution. The electrochromic material may exhibit several colors and can be termed as polyelectrochromic. Therefore remarkable effort has been performed for achieving new polymers which meet the criteria for commercial applications. To be used for electrochromic applications, some key issues such as long-term stability, rapid redox switching, high coloration efficiency (CE), and high optical transmittance change (Δ%T) during operation play important roles and are required to be achieved. Organic polymers with mechanical flexibility, and ease in band-gap/color-tuning via structural control, along with the potential for low-cost scalability and processing, are attractive in the fast-growing area of plastic electronics. For display devices, a polymer that can switch between opaque and transparent states is desirable as a polymer with a transparent conducting state being applicable in antistatic coating technology.

On the other hand, the near-infrared (NIR)-absorbing electrochromic materials are receiving great attention due to their potential applications in optical communications [4], biomedicine [5], camouflage materials in warfare [6], electro-optic switching in devices [7], thermal control and thermal emission detectors for spacecrafts [8]. However, compared with UV–visible absorbing materials, few NIR electrochromic materials have been developed to date [9].

Aromatic PIs are well-known as high-performance polymers that have excellent thermal, mechanical and electrical properties as well as outstanding chemical resistance [10–12]. However, the extremely high transition temperatures of the commercial PIs, which lie above their decomposition temperatures, and their poor solubility in common organic solvents give rise to processing difficulties and limit their applications [13,14]. These properties make them generally intractable or difficult to process; thus, their applications are restricted in some fields. As a consequence,

* Corresponding authors.
E-mail addresses: haijunniu@hotmail.com (H. Niu), wangwen@hit.edu.cn (W. Wang).
[1] These authors contributed equally to this paper.

0013-4686/$ – see front matter © 2013 Elsevier Ltd. All rights reserved.
http://dx.doi.org/10.1016/j.electacta.2013.08.160

recent basic and applied research has focused on enhancing their processability and solubility to broaden the scope of the technological applications of PIs while maintaining their excellent properties [15]. Attempts to increase the solubility and processability of PIs without sacrificing high thermal stability employed a variety of methods to chemically modify their structure, such as through the introduction of triphenylamine group into the polymer backbone [16–20], which as a structural modification to the rigid PIs has the potential to form an amorphous structure exhibiting excellent solubility and film-forming capabilities. In this method, triphenylamine (TPA) derivatives with the bulky propeller-shaped molecular structure are usually used, and they increase solubility and decrease intermolecular aggration dramastically [21].

The triarylamine unit is easy to be oxidazed in the nitrogen center and has the excellent ability to transport charge carriers via the radical cation species which have high stability and low ionization potential [22]. The compounds containing triarylamine are widely investigated and applied in various electro-optical materials such as organic light emitting diodes (OLEDs) [23], organic field-effect transistors [24], non-linear optical materials [25], and sensors [26], dye-sensitized solar cell (DSSCs) [27]. From the year of 2005, Liou et al. have investigated deeply on a series of TPA-based high-performance polyimides, polyamides, polyazomethines with attractive electrochromic properties bearing TPA derivatives such as N,N′-bis(4-aminophenyl)-N,N′-diphenyl-1,4-phenylenediamine [28], N,N′-bis(4-aminophenyl)-N,N′-diphenyl-1,4-phenyle nediamine, and other substituted TPAs [21]. All the PIs exhibited excellent electrochromic stability. When scanning potentials were varied from 0 V to 1.35 V, the PIs changed the color from the initial pale-yellowish at neutral form, to green, then to final blue at oxidized form gradually. It was found that the polymers based on TPA as core exhibited stable electrochromic characteristic, and the incorporation of electron-donating substituents at the para positions of triarylamines afforded stable radical cations.

In our ongoing effort to develop electrochromic polymeric materials, we have synthesized and investigated a series of high-performance polymers containing triphenylamine (TPA) [29], which showed good electrochromic reversibility in the visible region. In this contribution, we synthesized the diamine monomer N,N′-bis(4-aminophenyl)-N,N′-di-1-naphthalenyl-[1,1′-biphenhyl]-4,4′-diamine. PIs as thermally stable microelectronic materials have attracted great interest. Thus, we anticipated that the prepared electroactive PIs would reveal multi-electrochromic behaviors, high-electrochemical stability, improved optical response times, and enhanced contrast of optical transmittance in NIR region. Lastly, investigation of the energy levels for the PIs was done using theoretical analysis based on molecular orbital theory.

2. Experimental

2.1. Materials

N,N′-di(1-naphthyl)-4,4′-benzidine, was bought from Qinhuandao Bright Chemical Co. LTD, 4,4′-oxydiphthalic anhydride, 4,4′-biphthalic anhydride, 3,3′,4,4′-benzophenonetetracarboxylic dianhydride were purchased from TCI Co.; pyromellitic dianhydride, 4,4′-(hexafluoro isopropylidene) diphthalic anhydride; Pd/C(10%) were purchased from Acros; 4-fluoronitrobenzene, *N,N*-dimethylformamide (DMF) were supplied from Sinopharm Chemical Reagent Co., Ltd., China and used as received.

2.2. Synthesis of monomers

N,N′-bis(4-aminophenyl)-N,N′-di-1-naphthalenyl-[1,1′-biphenhyl]-4,4′-diamine (3) were synthesized with modified method in accordance with the literature [29] in Supporting Information (Scheme 1).

2.3. Synthesis of polymers

Preparation of PIs Pa-Pe by Two-Step Method via *Thermal Imidization Reaction.* The synthesis of Pc was used as an example to illustrate the general synthetic route. To a solution of 0.4120 g (0.67 mmol) of diamine **3** in 6.0 mL of DMF, 0.2070 g (0.67 mmol) of 4,4′-oxydiphthalic dianhydride c was added in one portion. Thus, the solid content of the solution is approximately 10 wt%. The mixture was stirred at room temperature for about 6 h to afford a viscous poly(amic acid) solution. The poly(amic acid) film was obtained by casting from the reaction polymer solution onto a glass plate and drying at 90 °C overnight under vacuum. The inherent viscosity of polyamic acid of Pc was 0.80 dL/g in DMF at a concentration of 0.5 g/dL at 30 °C. The polyamic acid in the form of film was converted to PI by successive heating under vacuum at 100 °C for 1 h, 200 °C for 1 h, and then 280 °C for 30 min. PIs (b–e) were prepared by an analogous procedure.

^{1}H NMR(400 MHz, DMSO-d_6, ppm, polyamic acid solid): 10.32–10.53 (m, the terminal groups of polyamide), 8.23–8.29 (the amide group), 6.71–7.76(aromatic ring of benzene).

FTIR spectrum (KBr pellet, PI): 1778 cm^{-1} (asymmetrical C═O), 1721 cm^{-1} (symmetrical C═O), 1664 cm^{-1} (amide carbonyl), 1392 cm^{-1} (C—N).

Polymer Pa. monomer **3** feed 0.2067 g (3.3×10^{-4} mol); pyromellitic dianhydride (a) 0.0726 g (3.3×10^{-4} mol); FTIR spectrum (KBr pellet): 1777, 1723, 1664, 1593, 1492, 1393.

Polymer Pb. Monomer **3** feed 0.2063 g (3.3×10^{-4} mol); 4,4′-biphthalic dianhydride (b) 0.0982 g (3.3×10^{-4} mol); FTIR spectrum (KBr pellet): 1775, 1719, 1663, 1600, 1490, 1391.

Polymer Pd. monomer **3** feed 0.2071 g (3.3×10^{-4} mol); 3,3′,4,4′-benzophenonetetracarboxylic dianhydride (d) 0.01076 g (3.3×10^{-4} mol); FTIR spectrum (KBr pellet):1777, 1718, 1669, 1579, 1503, 1388.

Polymer Pe. monomer **3** feed 0.2068 g (3.3×10^{-4} mol); 4,4′-(hexafluoro isopropylidene) dianhydride (e) 0.1479 g (3.3×10^{-4} mol); DMF 3 ml; FTIR spectrum (KBr pellet):1785, 1721, 1663, 1600, 1491, 1389.

2.4. Measurements

FT-IR spectra were recorded on a PerkinElmer Spectrum 100 Model FT-IR spectro meter. ^{1}H NMR spectra were measured on a Bruker AC-400 MHz spectrometer in DMSO-d_6, using tetramethylsilane as an internal reference. Thermogravimetric analysis (TGA) was conducted with a PerkinElmer Pyris 6 TGA. Experiments were carried out on approximately 6–8 mg powder samples heated in flowing nitrogen or air (flow rate = 20 cm^3/min) at a heating rate of 10 °C/min. DSC analyses were performed on a PerkinElmer Pyris diamond DSC at a scan rate of 10 °C/min in flowing nitrogen (20 cm^3/min). UV–vis-NIR absorption spectra were recorded using a SHIMADZU UV-3600 spectrophotometer whereas the photoluminescence solution spectra were registered on a Jasco FP-6200 spectrometer with 450 W Xenon lamp as the light source. The emission spectra of PIs were taken at λ_{exc} being equal to about the wavelength of the absorption maximum.

Cyclic voltammetry (CV) measurements were conducted on a CH Instruments 660A electrochemical analyzer at a scan rate of 50 mV s^{-1} with a 0.1 mol L^{-1} solution of $LiClO_4$ as an electrolyte under nitrogen atmosphere in dry acetonitrile (CH_3CN). The

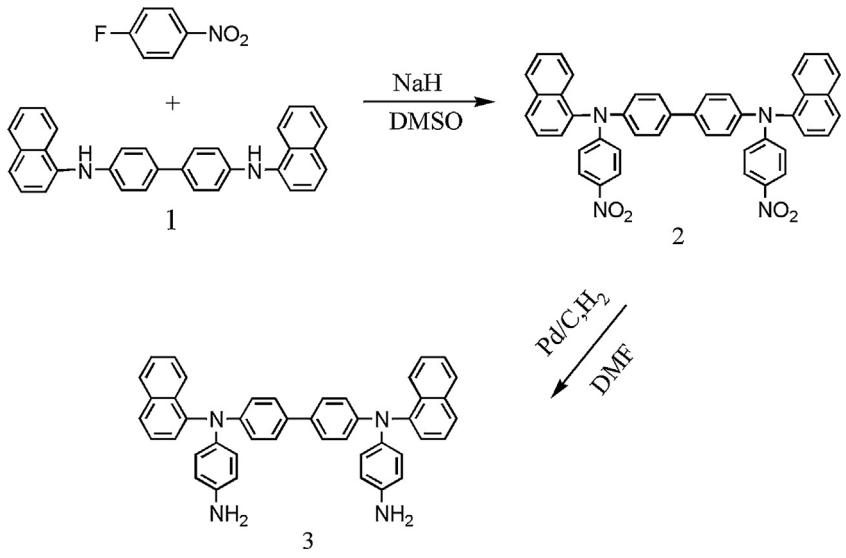

Scheme 1. Synthesis of Monomers.

oxidation and reduction potentials of polymer film coated on an ITO (indium tin oxide, $In_2O_3SnO_2$) disk were measured using a Pt wire and an Ag/AgCl electrode as a counter electrode and a quasi reference electrode, respectively. Under these conditions, the onsets of oxidation and reduction potentials of the polymer thin films against the Ag/AgCl quasi reference electrode were measured and calibrated against the ferrocene/ferrocenium (Fc/Fc^+) redox couple. For the electrochromic investigations, the PI film was cast on an ITO-coated glass slide, and a homemade electrochemical cell was built from a commercial ultraviolet (UV)-visible cuvette. The cell was placed in the optical path of the sample light beam in a UV–vis-NIR spectrophotometer, which allowed us to acquire electronic absorption spectra under potential control in a 0.1 mol L^{-1} $LiClO_4$/MeCN solution. The highest-occupied molecular orbital (HOMO) and lowest-unoccupied molecular orbital (LUMO) energy levels of the polymers were calculated by assuming the absolute energy level of Fc/Fc^+ as −4.80 eV to vacuum.

3. Results and discussion

3.1. Synthesis of monomers

Monomer was synthesized according to the procedure reported [29]. Diamine 3 is synthesized by the nucleophilic amination of aromatic amine and 4-fluoro-1-nitrobenzene under nucleophilic displacement conditions using a base NaH. Reduction of the dinitro intermediates was carried out using 10% Pd/C in DMF in autoclave with high pressure H_2 and resulted in a near quantitative yield of diaminotriphenylamine derivatives without toxicity to atmosphere by using hydrazine or tedious process by using $SnCl_2$. Especially, the higher pressure of H_2 can convert the raw materials to be soluble in the solution to get rid of catalysts.

3.2. Synthesis of polymers

The PIs were synthesized from diamine 3 and five commercially available dianhydrides a-e via a typical two step polymerization method. The structures and codes of the prepared polymers together are shown in Scheme 2. Structural characterization was conducted with the aid of IR spectroscopy (shown in Fig. S1) and the formation of poly(amic acid)s was confirmed with ^1H NMR spectroscopy (shown in Fig. S2). The characteristic absorptions for imide ring appear at 1777, 1720 (imide C=O), and 1390 cm^{-1} (C—N). Bands of amide groups appear at 1664 cm^{-1} (C=O).

3.3. Thermal properties

These PIs were obtained in almost quantitative yields, with inherent viscosities in the range of 0.75–0.84 dL/g, as shown in Table 1. All the polymers indicated no clear melting endotherms up to the decomposition temperatures on the DSC thermograms. Compared with the analogous PIs, because of the decreased conformational flexibility or free volume caused by the introduction of planar napthalene groups in the repeat unit, the series of PIs did not show clear T_g, but showed an enhanced thermal stability (Fig. 1).

Table 1
Thermal properties and inherent viscosity of the PIs.

	5 %	20 %	50 %	Char yield (%)	Poly(amic acid) η(dL/g)[a]
Pa	489	578	>800	65	0.84
Pb	514	616	>800	71	0.75
Pc	500	579	>800	64	0.80
Pd	519	>750	>800	81	0.78
Pe	531	628	>800	72	0.76

[a] Measured at a polymer concentration of 0.5 g/dL in DMF at 30 °C.

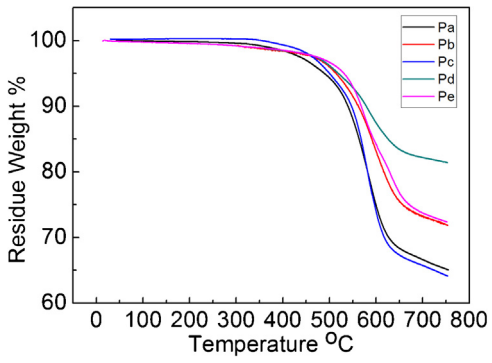

Fig. 1. TG diagrams of Pa to Pe.

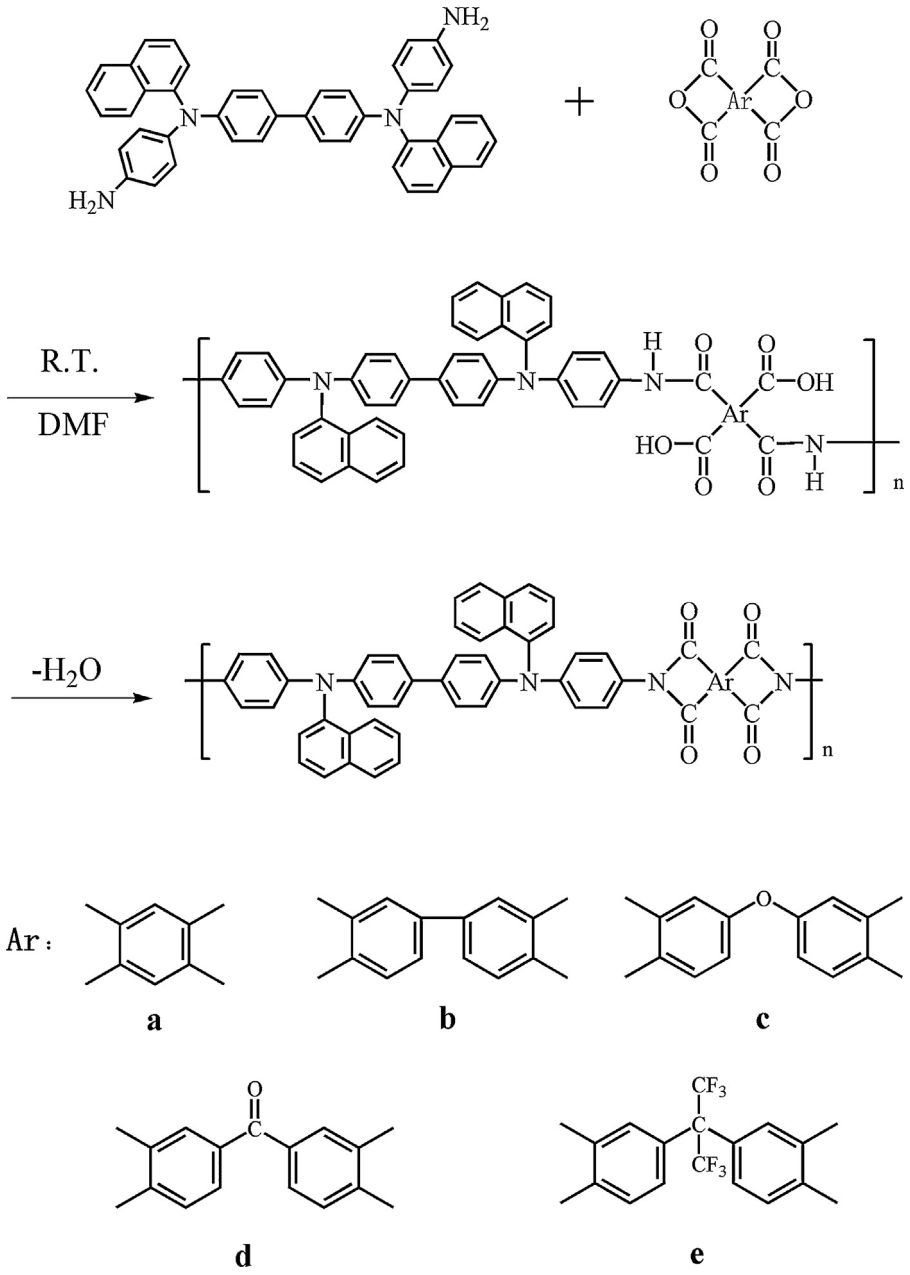

Scheme 2. Synthesis of PIs.

Fig. 1 depicts a typical set of TGA curves for Pa-Pe in nitrogen. The decomposition temperatures (T_d) at 5% and 20% weight losses in nitrogen were taken from the original TGA thermograms and are given in Table 1. All the prepared PIs exhibited good thermal stability with insignificant weight loss up to 450 °C under nitrogen atmosphere. The 5% weight loss temperatures of these polymers in nitrogen were recorded in the range of 489–531 °C. The amount of carbonized residues (char yield) at 750 °C in nitrogen for all PIs was in the range of 64–81 wt%. The high char yields of these PIs can be attributed to their high aromatic content. The lowest T_d value of Pc could be explained in terms of the ether bond segment in its backbone. Thus, the thermal analysis results revealed that these PIs exhibit excellent thermal stability, which in turn is beneficial to increase the service time in device application and to enhance the morphological stability of the spin-coated film.

3.4. Optical and electrochemistry properties

The optical properties of the polymers were investigated by UV–vis-NIR and photoluminescence spectroscopy. The results are summarized in Table 2. PL quantum yields φ of the samples in DMF were measured by using quinine sulfate dissolved in 0.1 mol L^{-1} sulfuric acids as a reference standard ($\varphi = 0.546$). The φs of these polymers after refractive index correction can be calculated according to the following eq [30]:

$$\phi_{unk} = \phi_{std}\left(\frac{I_{unk}}{I_{std}}\right)\left(\frac{A_{std}}{A_{unk}}\right)\left(\frac{\eta_{unk}}{\eta_{std}}\right)^2$$

where ϕ_{unk}, ϕ_{std}, I_{unk}, I_{std}, A_{unk}, A_{std}, η_{unk}, and η_{std} are the fluorescent quantum yield, integration of the emission intensity, absorbance at the excitation wavelength, and the refractive indices of the

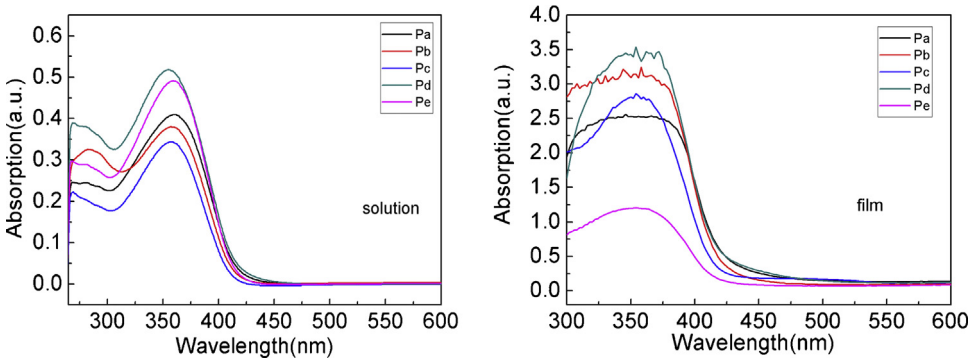

Fig. 2. UV–visible absorption spectra of PIs.

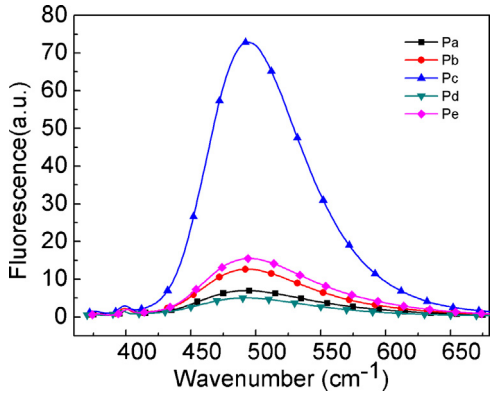

Fig. 3. PL spectra of PIs (in DMF solution, concentration: 10^{-6} mol L^{-1}).

corresponding solutions for the samples and the standard, respectively. Here, we use the refractive indices of the pure solvents as those of the solutions. Fig. 3 shows the PL spectra of PIs measured in DMF. Their PL spectra in DMF solution showed emission maximum around 491–493 nm (in the blue-green region), with a very low fluorescence quantum yields. These polymers exhibited strong UV–vis absorption bands in the range of 352–360 nm in DMF solution and in the range of 352–357 nm for solid film shown in Fig. 2, assignable to the π–π* transitions resulting from the conjugated TPA segment. Optical band gaps (E_g) determined from the absorption edge of the solid-state spectra of polymers are found to be 2.98–3.00 eV.

The typical cyclic voltammograms of Pa are shown in Fig. 4 The CV diagram indicates two well-defined redox waves, with half-wave potentials ($E_{1/2}$) of 0.72 and 0.935 V. The first peak, at 0.97 V, can be ascribed to oxidation of the electron-rich nitrogen atom in the TPA core. The second peak at 1.21 V, can be attributed to the formation of the TPA^{2+} radical ion, causing radical recombination and formation of a quinoid structure. In the CVs, the redox peaks have been associated with reduction–oxidation process accompanying the double injection/extraction of anion, $(ClO_4)^-$ and electrons. Because of the stability of the films and good adhesion between the polymer and ITO substrate, the Pa exhibited excellent reversibility of electrochromic characteristics by four continuous cyclic scans between 0.0 and 1.60 V. All of the polymers exhibited similar electrochromical properties. Similar spectral changes were observed for other PIs of this series (see the Fig. S3 in supporting information).

The energy levels of HOMO and LUMO of the investigated polymers can be determined from the oxidation onset potentials (E_{onset}) or half-wave potentials ($E_{1/2}$) and the onset absorption wavelengths, and the results are listed in Table 2. As a result, the HOMO energy values were calculated using the equation [31].

$$E_{HOMO} = -e(E_{ox\ vs\ Ag/AgCl} + 4.35)\,eV$$

where E_{ox} is the onset oxidation potential vs Ag/AgCl.

The HOMO energy values of Pa to Pe were calculated to be at in the range from −4.951 to −5.004 eV. Due to the reduction curves could hardly be obtained, the LUMO energy levels of the polymers were at between −1.971 (Pa) to −2.013 (Pe) eV estimated from the HOMO energy levels and E_g using the equations:

$$E_{LUMO} = E_{HOMO} + E_g^{opt}$$

$$E_g^{opt}\ (eV) = \frac{1240}{\lambda_{onset}\,(nm)}$$

In the PIs containing the same amine monomer, Pa showed the highest HOMO, and the Pc exhibited the lowest HOMO. The regularity was the same as that of UV–visible absorption. The different dianhydride structure played the key role in the electron structure and regulated the gaps of PIs. The lower ionization potential could suggest hole be easy injected into PI films from ITO electrodes in electronic device applications.

3.5. Spectroelectrochemical and electrochromic properties

Electrochromic behaviors of these PI thin films were examined by use of an optically transparent thin-layer electrode coupled with UV–vis-NIR spectroscopy. The typical absorption spectral changes of Pa were shown in Fig. 5, which exhibited that λ_{max} value for the π–π* transition of Pa was centered at 345 nm. In the neutral form,

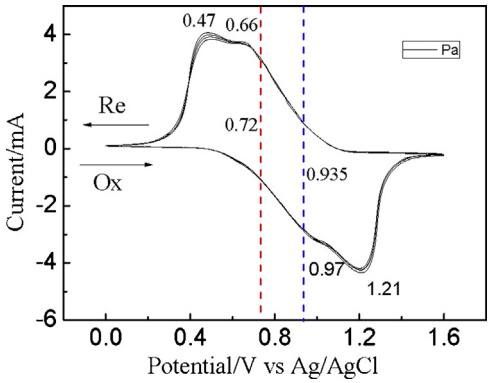

Fig. 4. Cyclic voltammograms for Pa in CH_3CN/0.1 mol L^{-1} $LiClO_4$ with Fc/Fc^+ as an internal standard, at 50 mV s^{-1}.

Table 2
Optical and electrochemical properties for PIs.

	λ_{film}^{abs} (nm)[a]	$\lambda_{solution}^{PL}$ (nm)[a]	λ_{onset}^{abs} (nm)[b]	ϕ^{c} (DMF)%	E^{peak} vs Ag/AgCl [d]	E_{onset}^{peak} vs Ag/AgCl	$E_{HOMO}^{electro}$ (eV)[f]	$E_{LUMO}^{electro}$ (eV)[f]	E_g^{film} (eV)[e]	E_{HOMO}^{quntum} (eV)[g]	E_{LUMOH}^{quntum} (eV)[g]	E_g^{quntum} (eV)[g]
Pa	354	492	416	0.090	0.720	0.6013	−4.951	−1.970	2.980	−4.861	−3.799	1.062
Pb	354	492	414	0.169	0.842	0.6320	−4.982	−1.986	2.995	−4.809	−3.424	1.384
Pc	355	493	413	0.936	0.833	0.6539	−5.003	−2.001	3.002	−4.821	−3.081	1.740
Pd	357	491	416	0.049	-	0.6225	−4.972	−1.991	2.980	−4.776	−3.816	0.959
Pe	352	493	415	0.164	-	0.6512	−5.001	−2.013	2.987	−4.828	−3.444	1.384

[a] UV–vis absorption and PL spectra measurements in DMF at room temperature.
[b] λ_{onset} of the polymer film.
[c] The quantum yield was calculated with quinine sulfate as the standard (φ = 54.6%).
[d] $E_{1/2}$: average potential of the redox couple peaks.
[e] $E_g = 1240/\lambda_{onset}$.
[f] The HOMO energy levels were calculated from cyclic voltammetry and were referenced to ferrocene (4.8 eV). $E_{LUMO} = E_{HOMO} - E_g$. $E_{ox/onset\,(Fc/Fc\text{-}vs.Ag/AgCl)} = 0.45$ V.
[g] Theoretical calculation of the polymers.

Fig. 5. Electrochromic behavior of Pa thin film (in CH_3CN with 0.1 mol L^{-1} $LiClO_4$ as the supporting electrolyte) at 0.0, 0.8, 0.9, 1.0,1.1, 1.15, 1.2, 1.25, 1.3, 1.35, 1.4, 1.45, 1.5 (V vs. Ag/AgCl). The inset shows the photographic images of the film at different applied voltages.

at 0 V the film exhibited strong absorption at wavelength around 345 nm, characteristic for triarylamine, but it was almost transparent in the visible region. Upon oxidation of the **Pa** film (increasing applied voltage from 0 to 1.3 V), the intensity of the absorption peak at 345 nm gradually decreased while a new peak at 479 nm and a broad band having its maximum absorption wavelength at 1332 nm in the NIR region gradually increased in intensity. We attribute the spectral change in visible range to the formation of a stable monocation radical of the TPA center in diamine **3** moiety. Furthermore, the broad absorption in NIR region was the characteristic result due to IV-CT (leading an intervalence charge transfer) excitation associated with IET (Intramolecular electron transfer) from active neutral nitrogen atom to the cation radical nitrogen center of diamine **3** moiety, which was consistent with the phenomenon classified by Robin and Day [32]. As the applied potential became more anodic to 1.5 V, the absorption bands of the cation radical decreased gradually in intensity, with the formation of a new broadband centered at around 895 nm. The disappearance of NIR absorption band can be attributable to the further oxidation of monocation radical species to the formation of dication in the diamine **3** segments. The observed UV–vis-NIR absorption changes in the film of Pa at various potentials are fully reversible and are associated with strong color changes; indeed, they even can be seen readily by the naked eye. From the inset shown in Fig. 5, it can be seen that the film of polymer Pa switched from a transmissive neutral state (pale yellow) to a highly absorbing semioxidized state (red) and a fully oxidized state (blue). The other polymers showed similar spectral changes to that of Pa (see the Fig. S4 in supporting information).

3.6. Electrochromic Switching Studies

Because of the apparent high electrochromic contrast, optical switching studies were investigated more deeply to manifest the outstanding electrochromic characteristics of these obtained novel anodically electrochromic materials. For optical switching studies, the polymer films were cast on ITO-coated glass slides in the same manner as described above, and each film was potential stepped between its neutral (−0.2 V) and oxidized (1.2 V) state. As the films were switched, the absorbance at the given wavelength was monitored as a function of time with UV–vis-NIR spectroscopy. Switching data for the representative cast film of PI Pe are shown in Fig. 6. The switching time is defined as the time required for reach 90% of the full change in absorbance after the switching of the potential. As depicted in Fig. 6, polyimides Pe thin film revealed switching time of 1.12 s at 1.20 V for coloring process at 479 nm and 0.93 s for bleaching. The polyimides switched rapidly between the

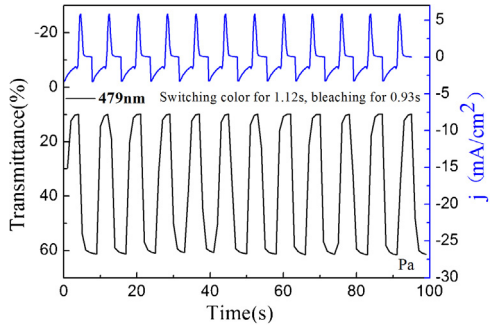

Fig. 6. Dynamic changes of the transmittance and current upon switching the potential between −0.2 ↔ 1.2 V (vs. Ag/AgCl) with a pulse width of 8 s applied to the cast film of polymer Pe on the ITO-coated glass slide in MeCN containing 0.1 mol L^{-1} $LiClO_4$. The absorption was recorded at 479 nm.

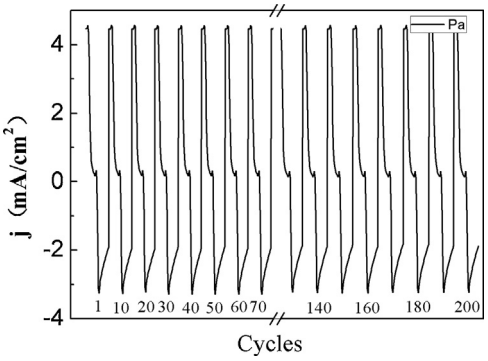

Fig. 7. Current consumption between −0.2 ↔ 1.2 V (vs. Ag/AgCl) of polymer Pa thin film on the ITO-coated glass substrate in a 0.1 mol L^{-1} $LiClO_4/CH_3CN$ solution with a cycle time of 8 s.

highly transmissive neutral state and the colored oxidized state. The electrochromic stability of the Pe film was also determined by measuring the optical change as a function of the number of switching cycles(the others in Fig. S5).

The electrochromic coloration efficiency (CE; η) is also an important characteristic for the electrochromic materials. CE can be calculated using the equations and given below [33]:

$$\delta_{OD} = lg\left(\frac{T_b}{T_c}\right) \quad \text{and} \quad \eta = \frac{\delta_{OD}}{Q}$$

where T_b and T_c are the trans mittances before and after coloration, respectively. δ_{OD} is the change of the optical density, which is proportional to the amount of created color centers. η denotes the coloration efficiency(CE). Q (mC/cm^2) is the amount of injected/ejected charge per unit sample area. CE of Pd film is measured as 1069.73 cm^2/C (at 479 nm) at full doped state, which had reasonable coloration efficiency (the others in Table 3).

After over continuous 200 cyclic switches between −0.2 and 1.2 V, the polymer films still exhibited good stability of electrochromic characteristics(shown in Fig. 7 and the others in Fig. S6).

3.7. Photoelectrochemical activity

A steady anodic photocurrent was obtained from the dye monolayer-modified electrode when the PI-ITO electrode was illuminated, by white light under 150 mW cm^{-2} light intensity and without any bias voltage, in 0.1 M $LiClO_4$ electrolyte solution. The photoelectric response was very stable when switching on and off many times, as shown in Fig. 8. For comparison, the bare ITO did not exhibit the phenomena suggesting that the PI is responsible for photocurrent generation.

Fig. 8(b) showed typical open-circuit photovoltaic response of electrode on illumination at different voltage biases. After the light being turned on was turned off, the photovoltage decayed to lowest slowly. On the contrast, after the light was being turned off, the photovoltage increased instantly. This observation was consistent with the injection of electrons from the LUMO of the Pa to the conduction band of the ITO surface.

Table 3
Optical and electrochemical data collected for coloration efficiency measurements of polyimides.

Polymer code[a]	λ (nm)[b]	δ_{OD}[c]	Q (mC/cm^2)[d]	η (cm^2/C)[e]
Pa	479	0.7979	5.2020	153.38
Pb	476	0.6098	5.8596	104.06
Pc	479	0.966	2.415	400
Pd	477	0.8948	4.085	219.04
Pe	479	0.7320	0.68248	1069.73

[a] Switching between −0.20 and 1.20 for Pa-Pe (V vs. Ag/AgCl).
[b] Given wavelength where the data were determined.
[c] Optical density change at the given wavelength.
[d] Ejected charge is determined from the in situ experiments.
[e] Coloration efficiency is derived from the equation $\eta = \delta_{OD}/Q$.

3.8. Quantum chemistry calculation

In order to obtain deeper insight into the polymer structure–property relationships, ground-state geometry optimizations and energy levels of the evolution of the oxidation and reduction potentials, the electronic structures of the oligomer of PIs were carried out by using density functional theory at the B3LYP/6-31G level.

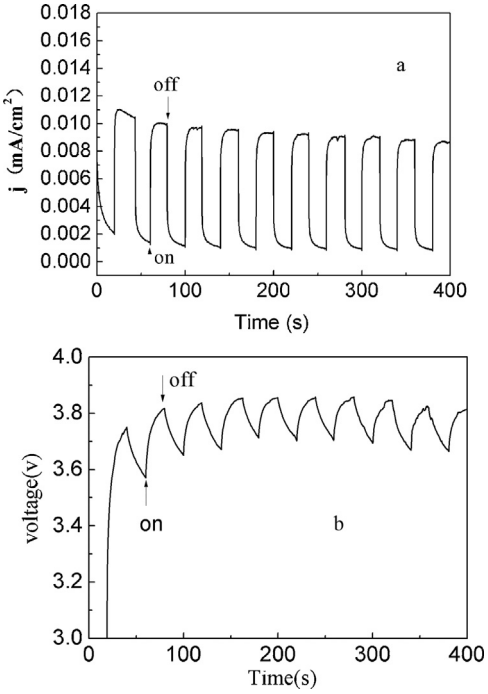

Fig. 8. A typical photocurrent (a) and photovoltagic (b) response for Pa immobilized ITO glass upon exposure to on/off light at room temperature.

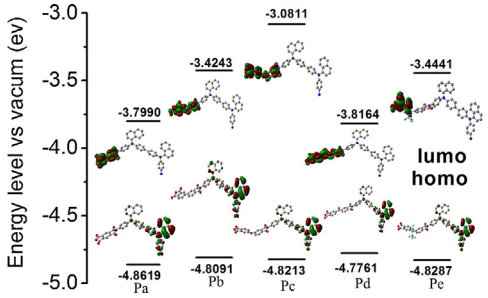

Fig. 9. Pictorial representations of the electron density in the frontier molecular orbitals of repetition units for Pa to Pe in the order.

The HOMO and LUMO energy level and HOMO–LUMO energy gaps (E_g) are given in Table 2. Pictorial representations of the frontier molecular orbitals of the polymers are shown in Fig. 9, which illustrate that the electron density distribution of the HOMO state of the basic unit (ground state) was mainly located on triphenylamine moiety representing for electronic state of the first oxidation state, and that of the LUMO state of the basic unit was mainly located on dianhydride moiety.

The theory trend of E_g for the oligomer series follows in the order: Pd <Pa < Pe < Pb < Pc which basically corresponds with the experimental data in the order: Pd = Pa < Pe < Pb < Pc (Table 2). It should be noted that the calculated results are based on monomer unit. In fact, the experiment data are obtained from oligomers or polymers which are influenced by the solvent and electrolyte and more complicated.

4. Conclusion

We succeeded in taking the strategic to tune the band gap of PIs by copolymerization with five different dianhydrides. The resultant PIs show excellent thermal resistance, good solubility in many organic solvents such as DMSO, DMF, DMAc, NMP which can be cast to be film. The PIs show the color in yellow, but after electrooxidation, the colors change to blue, which means the PIs can be used in sensors, solar cell, and flexible electronic devices. We investigated the relationship of the structure and the optical properties by experiment and theory, and found that the experiment results conformed to the quantum chemical calculation well. Thus, these characteristics suggest that these new polyimides have great potential for use in optoelectronics applications.

Acknowledgement

The authors are grateful to the support of the Foundation of Heilongjiang Education Bureau (12531504), the National Science Foundation of China (Grant Nos. 51373029, 51372055), Doctoral Fund of Ministry of Education of China. Heilongjiang University Graduate-student Innovation Scientific Research Projects, Foundation of Heilongjiang University Innovator Group (No. hdtd-2010-11).

Appendix A. Supplementary data

Supplementary data associated with this article can be found, in the online version, at http://dx.doi.org/10.1016/j.electacta.2013.08.160.

References

[1] H. Shin, Y. Kim, T. Bhuvana, J. Lee, X. Yang, C. Park, E. Kim, Color combination of conductive polymers for black electrochromism, ACS Appl. Mater. 4 (2012) 185.
[2] C.J. Yao, Y.W. Zhong, H.J. Nie, H.D. Abruña, J.N. Yao, Near-IR electrochromism in electropolymerized films of a biscyclometalated ruthenium complex bridged by 1,2,4,5-tetra(2-pyridyl)benzene ligand, J. Am. Chem. Soc. 133 (2011) 20720.
[3] S. Beaupre, J. Dumas, M. Leclerc, A variable optical attenuator operating in the near-infrared region based on an electrochromic molybdenum complex, Chem. Mater. 18 (2006) 4011.
[4] A.M. McDonagh, S.R. Bayly, D.J. Riley, M.D. Ward, J.A. McCleverty, M.A. Cowin, C.N. Morgan, R. Varrazza, R.V. Penty, I.H. White, A variable optical attenuator operating in the near-infrared region based on an electrochromic molybdenum complex, Chem. Mater. 12 (2000) 2523.
[5] S. Xun, G. LeClair, J. Zhang, X. Chen, J.P. Gao, Z.Y. Wang, Tuning the electrical and optical properties of dinuclear ruthenium complexes for near infrared optical sensing, Org. Lett. 8 (2006) 1697.
[6] G. Sönmez, P. Schottland, K. Zong, J.R. Reynolds, Highly transmissive and conductive poly[(3,4alkylenedioxy)pyrrole2,5diyl] (PXDOP) films prepared by air or transition metal catalyzed chemical oxidation, J. Mater. Chem. 11 (2001) 289.
[7] C.S. Grange, A.J.H.M. Meijer, M.D. Ward, Trinuclear ruthenium dioxolene complexes based on the bridging ligand hexahydroxytriphenylene: electrochemistry, spectroscopy, and near-infrared electrochromic behaviour associated with a reversible seven-membered redox chain, Dalton Trans. 39 (2010) 200.
[8] P. Chandrasekhar, G.C. Birur, P. Stevens, S. Rawal, E.A. Pierson, K.L. Miller, P. Chandrasekhar, G.C. Birur, P. Stevens, S. Rawal, E.A. Pierson, K.L. Miller, Far infrared electrochromism in unique conducting polymer systems, Synth. Met. 119 (2001) 293.
[9] (a) Y. Zheng, J. Cui, J. Zheng, X. Wan, Near-infrared electrochromic and chiroptical switching polymers: synthesis and characterization of helical poly(N-propargylamides) carrying anthraquinone imide moieties in side chains, J. Mater. Chem. 20 (2010) 5915;
(b) G. Qian, H. Abu, Z.Y. Wang, A precursor strategy for the synthesis of low band-gap polymers: an efficient route to a series of near-infrared electrochromic polymers, J. Mater. Chem. 21 (2011) 7678.
[10] S.H. Cheng, S.H. Hsiao, T.H. Su, G.S. Liou, Novel electrochromic aromatic poly(amine- amide-imide)s with pendent triphenylamine structures, Polymer 46 (2005) 5939.
[11] S.H. Hsiao, G.S. Liou, Y.C. Kung, H.Y. Pan, C.H. Kuo, Electroactive aromatic polyamides and polyimides with adamantylphenoxy-substituted triphenylamine units, Eur. Polym. J. 45 (2009) 2234.
[12] N.V. Sadavarte, C.V. Avadhani, P.V. Naik, P.P. Wadgaonkar, Regularly alternating poly(amideimide)s containing pendent pentadecyl chains: synthesis and characterization, Eur. Polym. J. 46 (2010) 1307.
[13] H.R. Kricheldorf, B. Schmidt, New polymer syntheses. 68. Kevlar-type polyaramides derived from 2-phenoxy-1,4-diaminobenzene Hans R. Kricheldorf; Bernd Schmidt, Macromolecules 25 (1992) 5471.
[14] H.R. Kricheldorf, R. Burger, New polymer syntheses. LXXV. 2,5-Biaryloxyterephthalic acids and rigid-rod polyaramides derived from them Hans R. Kricheldorf; Rolf Bürger, J. Polym. Sci., Part A: Polym. Chem. 32 (1994) 355.
[15] H.M. Wang, S.H. Hsiao, Electrochemically and electrochromically stable polyimides bearing tert-butyl-blocked N,N,N′,N′-tetraphenyl-1,4-phenylenediamine units, Polymer 50 (2009) 1692.
[16] S.J. Zhang, Y.F. Li, D.X. Yin, X.Y. Shao, S.Y. Yang, Study on synthesis and characterization of novel polyimides derived from 2,6-Bis(3-aminobenzoyl) pyridine, Eur. Polym. J. 41 (2005) 1097.
[17] Z.X. Hu, Y. Yin, H. Kita, K. Okamoto, Y. Suto, H.G. Wang, H. Kawasato, Zhaoxia Hu, Yan Yin, Hidetoshi Kita, Ken-ichi Okamoto, Yoshiki Suto, Honguan Wang, Hironobu, Kawasato, Synthesis and properties of novel sulfonated polyimides bearing sulfophenyl pendant groups for polymer electrolyte fuel cell application, Polymer 48 (2007) 1962.
[18] Y. Shao, Y.F. Li, X. Zhao, T. Ma, C.L. Gong, F.C. Yang, Synthesis and characterization of soluble polyimides derived from a novel unsymmetrical diamine monomer: 1,4-(2′,4″-diaminodiphenoxy)benzene, Eur. Polym. J. 43 (2007) 4389.
[19] H.S. Choi, I.S. Chung, K. Hong, C.E. Park, S.Y. Kim, Soluble polyimides from unsymmetrical diamine containing benzimidazole ring and trifluoromethyl pendent group, Polymer 49 (2008) 2644.
[20] M. Ghaemy, R. Alizadeh, Synthesis of soluble and thermally stable polyimides from unsymmetrical diamine containing 2,4,5-triaryl imidazole pendent group, Eur. Polym. J. 45 (2009) 1681.
[21] Y.C. Kung, W.F. Lee, S.H. Hsiao, G.S. Liou, New polyimides incorporated with diphenylpyrenylamine unit as fluorophore and redox-chromophore, J. Polym. Sci., Part A: Polym. Chem. 49 (2011) 2210.
[22] A. Iwan, D. Sek, Polymers with triphenylamine units: photonic and electroactive materials, Prog. Polym. Sci. 36 (2011) 1277.
[23] M. Thelakkat, Dendrimeric and polymeric triarylamines as photoconductors and hole transport materials for electro-optical applications, Macromol. Mater. Eng. 287 (2002) 442.
[24] B. Cho, S. Song, Y. Ji, T.W. Kim, T. Lee, Organic resistive memory devices: performance enhancement, integration, and advanced architectures, Adv. Funct. Mater. 21 (2011) 2806.

[25] S. Köber, M. Salvador, K. Meerholz, Organic photorefractive materials and applications, Adv. Mater. 23 (2011) 4725–4763.
[26] K. Ghosh, G. Masanta, R. Fröhlich, I.D. Petsalakis, Triphenylamine-based receptors in selective recognition of dicarboxylic acids, J. Phys. Chem. B 113 (2009) 7800.
[27] T. Bessho, S.M. Zakeeruddin, C.Y. Yeh, W.G. Eric Diau, M. Grätzel, Highly efficient mesoscopic dye-sensitized solar cells based on donor-acceptor-substituted porphyrins, Angew. Chem. Int. Ed. 49 (2010) 6646.
[28] G.S. Liou, S.H. Hsiao, M. Ishida, M. Kakimoto, Y. Imai, Synthesis and properties of new aromatic poly(amine-imide)s derived from N,N′-bis(4-aminophenyl)-N,N′-diphenyl-1,4-phenylenediamine, J. Polym. Sci., Part A: Polym. Chem. 40 (2002) 3815.
[29] (a) H.J. Niu, P.H. Luo, M.L. Zhang, L. Zhang, L.N. Hao, J. Luo, X.D. Bai, W. Wang, Multifunctional, photochromic, acidichromic, electrochromic molecular switch: novel aromatic poly(azomethine)s containing triphenylamine group, Eur. Polym. J. 45 (2009) 3058;
(b) H.J. Niu, H.Q. Kang, J.W. Cai, C. Wang, X.D. Bai, W. Wang, Novel soluble polyazomethines with pendant carbazole and triphenylamine derivatives: preparation, characterization and optical, electrochemical, electrochromic properties, Polym. Chem. 2 (2011) 2804;
(c) J.W. Cai, H.J. Niu, C. Wang, L.N. Ma, X.D. Bai, W. Wang, Tuning the bandgaps of polyazomethines containing triphenylamine by different linkage sites of dialdhyde monomers, Electrochim. Acta 76 (2012) 229.
[30] F.C. Tsai, C.C. Chang, C.L. Liu, W.C. Chen, S.A. Jenekhe, New thiophene-linked conjugated poly(azomethine)s: theoretical electronic structure, synthesis and properties, Macromolecules 38 (2005) 1958.
[31] C.H. Duan, W.Z. Cai, F. Huang, J. Zhang, M. Wang, T.B. Yang, C.M. Zhong, X. Gong, Y. Cao, Novel silafluorene-based conjugated polymers with pendant acceptor groups for high performance solar cells, Macromolecules 43 (2010) 5262.
[32] M. Robin, P. Day, Mixed valence chemistry—a survey and classification, Adv. Inorg. Radiochem. 10 (1968) 247.
[33] S.J. Yoo, J.H. Cho, J.W. Lim, S.H. Park, J. Jang, Y.E. Sung, High contrast ratio and fast switching polymeric electrochromic films based on water-dispersible polyaniline-poly(4-styrenesulfonate) nanoparticles, Electrochem. Commun. 12 (2010) 164.